Antitumor Agents

Deutsche Ausgabe: DOI: 10.1002/ange.201510866
Internationale Ausgabe: DOI: 10.1002/anie.201510866

Re-engineering the Immune Response to Metastatic Cancer: Antibody-Recruiting Small Molecules Targeting the Urokinase Receptor

*Anthony F. Rullo, Kelly J. Fitzgerald, Viswanathan Muthusamy, Min Liu, Cai Yuan, Mingdong Huang, Minsup Kim, Art E. Cho, and David A. Spiegel**

Abstract: *Developing selective strategies to treat metastatic cancers remains a significant challenge. Herein, we report the first antibody-recruiting small molecule (ARM) that is capable of recognizing the urokinase-type plasminogen activator receptor (uPAR), a uniquely overexpressed cancer cell-surface marker, and facilitating the immune-mediated destruction of cancer cells. A co-crystal structure of the ARM-U2/uPAR complex was obtained, representing the first crystal structure of uPAR complexed with a non-peptide ligand. Finally, we demonstrated that ARM-U2 substantially suppresses tumor growth in vivo with no evidence of weight loss, unlike the standard-of-care agent doxorubicin. This work underscores the promise of antibody-recruiting molecules as immunotherapeutics for treating cancer.*

Tumor metastasis involves the invasion of cancer cells into surrounding tissues, a process often accelerated by cell-surface proteases. One such protease, the urokinase-type plasminogen activator (uPA), breaks down extracellular matrix proteins and activates migration-inducing signal cascades upon binding to the urokinase-type plasminogen activator receptor (uPAR).[1] Both uPA and uPAR expression are substantially upregulated in invasive cancer cells compared to healthy cells or benign tumors.[2] In clinical settings, uPAR levels have been shown to correlate with metastatic potential and poor clinical outcomes.[1a] As such, uPAR has gained recognition as a promising target for treating metastatic cancers from diverse tissues of origin, including breast, colon, stomach, and bladder.[3,4]

[*] Dr. A. F. Rullo, Dr. V. Muthusamy, Prof. Dr. D. A. Spiegel
Department of Chemistry, Yale University
225 Prospect Street, New Haven, CT 06511 (USA)
E-mail: david.spiegel@yale.edu
K. J. Fitzgerald, Prof. Dr. D. A. Spiegel
Department of Pharmacology, Yale School of Medicine
333 Cedar Street, New Haven, CT 06520 (USA)
M. Liu, Dr. C. Yuan, Prof. Dr. M. Huang
State Key Laboratory of Structural Chemistry
Fujian Institute of Research on the Structure of Matter
Chinese Academy of Sciences
155 Yang Qiao West Road, Fuzhou, Fujian 350002 (China)
M. Kim, Prof. Dr. A. E. Cho
Department of Bioinformatics, Korea University
2511 Sejong-ro, Sejong, 339-700 (Korea)

Supporting information for this article is available on the WWW under http://dx.doi.org/10.1002/anie.201510866.

Antibody-recruiting molecules (ARMs) are bifunctional molecules capable of delivering endogenous antibodies to disease-causing entities, leading to their destruction and/or clearance by the immune system. Our group and others have previously developed ARMs that target various cancers and infectious agents. These novel immunotherapies have the potential both to complement protein-based agents while overcoming their challenges, such as poor oral bioavailability, high molecular weights, and immunogenicity.[5]

Our group previously reported an ARM capable of targeting uPAR-expressing cancer cells for immune-mediated cell death.[5] Although effective in vitro, the reported construct (termed ARM-U1) contained the uPA protein at its target binding terminus (TBT), imparting many of the limitations of biologics. We therefore hypothesized that the therapeutic potential of this agent could be significantly improved upon by replacing the uPA protein with a high-affinity uPAR-binding small molecule (Figure 1 A).

Herein, we report the design, synthesis, and in vitro and in vivo evaluation of a second-generation, low-molecular-weight (< 1000 amu) ARM derivative termed ARM-U2. In place of uPA, ARM-U2 incorporates a restructured analogue of IPR-803, a uPAR inhibitor identified previously using a virtual screen, into its TBT.[6] ARM-U2 targets the uPA binding site on uPAR with low nanomolar affinity, induces immune-mediated phagocytosis and cytotoxicity of uPAR-expressing cells in culture, and also inhibits tumor progression in vivo, possessing comparable efficacy to the standard-of-care agent doxorubicin but without the substantial weight loss associated with doxorubicin treatment. We also report a co-crystal structure of the ARM-U2/uPAR complex, which to our knowledge represents the first uPAR/small-molecule inhibitor complex to appear in the literature. This work underscores the promise of small-molecule immunotherapeutics for treating patients with uPAR-expressing metastatic cancers.

In designing ARM-U2, we first sought to identify a site in the IPR-803 scaffold at which to affix a linker connecting the TBT to a 2,4-dinitrophenyl (DNP) antibody-binding terminus (ABT). To this end, we performed computationally assisted docking experiments,[7] which suggested that functionalization of the IPR-803 core at position 2 of ring C with triethylene glycol derived PEG-3 linker **9** would be sufficient to drive solvent exposure of the ABT (**1**; Figure 1 B). Also, computational studies performed previously and in our laboratory suggested that electrostatic interactions between R53 and the carboxylate of IPR-803 are critical for driving

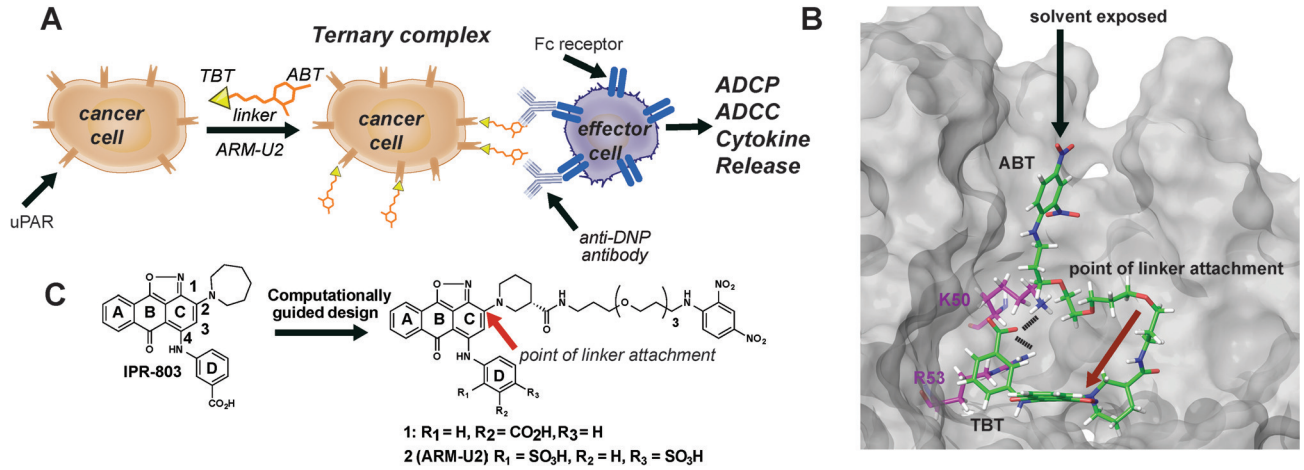

Figure 1. A) The reported antibody-recruiting small molecule (ARM) approach to targeting metastatic cancer cells that over-express uPAR. An ARM binds uPAR-expressing cancer cells, followed by the recruitment of anti-DNP antibodies to the cell surface, which in turn mediate a range of effector cell functions, including antibody-dependent cellular phagocytosis (ADCP) and cytotoxicity (ADCC). The bifunctional ARM-U2 is composed of an antibody-binding terminus (ABT), a linker region, and a uPAR-target-binding terminus (TBT). B) The docking of IPR-803-substituted derivative **1** to the crystal structure of uPAR. The ABT region remains solvent-exposed (black arrow) while the small molecule TBT is engaged in binding uPAR. Proposed interactions with residues R53 and K50 are indicated. C) The chemical structure of derivative **1** and derivative **2** (ARM-U2); the latter was predicted to display high-affinity uPAR binding.

ligand affinity.[8] We therefore hypothesized that repositioning this carboxylate function closer to R53, and/or incorporating additional acidic sites into the ligand, would improve its overall binding affinity. To test this, we performed further docking studies with model derivatives differing in the number or position of negatively charged substituents within ring D. We explored biscarboxylate **15**, extended monocarboxylate **16**, and the mono- and bissulfonate derivatives **17** and **2**, respectively (Figure 2). Compound **15** was predicted to bind uPAR with comparable affinity to **1**, whereas the other derivatives were calculated to have significantly stronger docking scores, likely both because of stronger electrostatic contacts and additional bonding interactions with the hotspot residues R53 and K50 (Table 1, Figure S1).

Informed both by these computational results and published SAR studies,[8] we prepared several candidate ARM-U2 derivatives for further evaluation (Figure 2). These were synthesized in a divergent manner starting from isoxazole **3** (Figure 2, Scheme S2).[8b] Thus, exposure of **3** to a diverse set of commercially available functionalized anilines under Lewis acid catalysis at ambient temperature led to the chemoselective displacement of the 4-bromo substituent to afford variously substituted intermediates **4**–**8** in high yields. Treatment of **4**–**8** with amine base and (*S*)-3-piperidinecarboxylate derivatives **9**–**12**, containing linkers of various lengths and antibody-binding motifs, led to a second displacement process of the bromine atom in the 2 position. Ester deprotection where appropriate yielded products **1**, **2**, and **13**–**20** in good to excellent yields.[8b]

We then evaluated the binding of compounds **1**, **2**, and **13**–**20** to uPAR using a competition ELISA protocol (Table 1). We first observed that the K_I and K_d values determined for **1** were in close agreement with the reported 200 nM affinity of

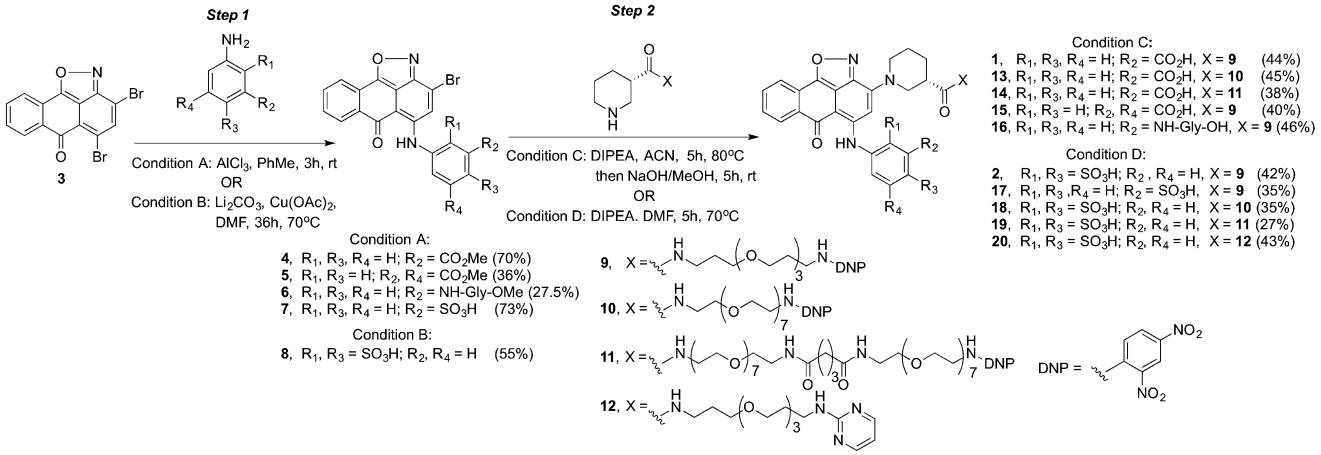

Figure 2. Chemical synthesis of the ARM-U candidate derivatives employed in this study.

Table 1: Docking scores and in vitro binding affinities calculated using a competitive ELISA binding assay for selected ARM-U candidate derivatives.

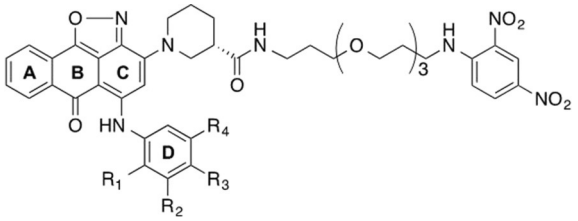

Entry	Compound	R_1	R_2	R_3	R_4	Docking [kcal mol^{-1}]	K_I[a] [nM]
1	**1**	H	CO_2H	H	H	−12.175	640 ± 180
2	**15**	H	CO_2H	H	CO_2H	−11.124	408 ± 22
3	**16**	H	NH-Gly-OH	H	H	−36.809	240 ± 39
4	**2**	SO_3H	H	SO_3H	H	−64.655	12 ± 1

[a] Values calculated from triplicate IC_{50} measurements using a competitive binding ELISA as described in the Supporting Information. Inhibitory constants calculated from the IC_{50} values generated using the Cheng–Prusoff equation as described in the Supporting Information.

IPR-803 for uPAR (see also Figure S2).[8a] This result supports computational predictions that linker ABT installation at position 2 of ring C would minimally perturb uPAR binding affinity. ARM-U candidates (**1**, **2**, and **13**–**20**) were also found to bind uPAR competitively with uPA possessing affinities ranging from low double- to triple-digit nanomolar values (Table 1, Table S1, and Figure S2). Although the absolute magnitudes of the computational docking energies did not correlate with experimental binding affinities, the highest ranked compound, bissulfonate **2**, was found to possess the highest uPAR binding affinity with a K_I value of 12 nM (Table 1). These binding results validated our hypothesis that repositioning and/or increasing the negative charge on the D ring of ARM-U2 derivatives could afford significant increases in uPAR binding affinity.

We next evaluated the ability of **1** and **2** (henceforth termed "ARM-U2") to induce responses from immune effector cells. We measured the antibody-dependent cellular phagocytosis (ADCP) of uPAR-expressing A172 glioblastoma cells by IFNγ-activated U937 monocytes using a two-color flow-cytometry procedure. Both **1** and ARM-U2 exhibited concentration-dependent phagocytosis with maximum efficacy observed at approximately 1 μM and 100 nM, respectively (Figure 3A, Figure S4). The bell-shaped, autoinhibitory dose-response curve observed at ARM-U2 concentrations greater than 100 nM has been termed the "prozone" effect, and is expected for agents that function through ternary complexes, as has been described in detail previously.[9] When present at high concentrations, unbound bifunctional agents compete with both antibody and cell-surface interactions in the ternary complex, driving the equilibrium to constituent binary complexes, thus preventing phagocytosis.

The dependence of ADCP on the presence of cell-surface uPAR was next assessed through competition experiments. Competition with soluble uPAR (suPAR) or **20**, an ARM-U derivative lacking the DNP function, substantially suppressed ARM-U2-mediated phagocytosis (Figures 3A, S4, and S6). ARM-U2 was also capable of eliciting antibody-dependent cellular cytotoxicity (ADCC), which was suppressed in the presence of competitors (Figure S4). Taken together, these results support that ARM-U2 is capable of inducing both ADCP and ADCC in a manner dependent on binding anti-DNP antibodies and cell-surface uPAR.

To further assay the effector cell activation by ARM-U2, we investigated the release of pro-inflammatory cytokines by U937 monocytes in the context of ADCP assays. Thus, cellular supernatants were isolated from ADCP assay conditions and evaluated using a multi-inflammatory cytokine ELISA protocol.

Higher levels of IL-8 secretion were observed in assays containing 50 nM or 1 μM ARM-U2 compared to control samples lacking ARM-U2 (Figure 3B). We believe that the slight decrease in IL-8 release at 1 μM versus 50 nM of ARM-U2 is another manifestation of the prozone effect, and coincides well with

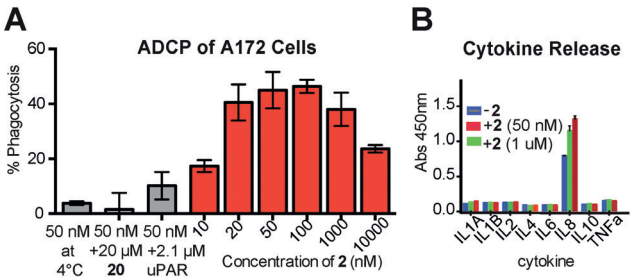

Figure 3. Demonstration of the in vitro efficacy and potency of ARM-U2 (**2**) in immune effector cell assays using A172 glioblastoma cells as targets. A) Antibody-dependent cellular phagocytosis (ADCP) of A172 glioblastoma cells in the presence of anti-DNP antibodies (133 nM) at the indicated concentrations of ARM-U2 (**2**) and competitor. Studies were conducted at both 37 °C and 4 °C and in the presence or absence of either exogenous uPAR or derivative **20**, as indicated. B) ARM-U2 induces the release of the inflammatory cytokine IL-8 from U937 cells in ADCP assays at concentrations of both 50 nM and 1 μM as shown.

the concentration dependence observed in the ADCP experiments shown in Figure 3A. These results are consistent with previous reports demonstrating that IL-8 is among the first cytokines released by monocytes and macrophages during the innate immune response, and serves as a downstream indicator of antibody-dependent cell-surface clustering and activation of CD64 (FcγRI).[10] Also, the apparent absence of other cytokines in these experiments likely results from our exclusive use of CD64-expressing monocytic effector cells.

To gain insight into the ARM-U2 binding mode, we obtained a co-crystal structure of ARM-U2 bound to the uPAR soluble extracellular domain (suPAR).[11] These studies revealed that ARM-U2 binds in a deep hydrophobic pocket within the uPA binding site on uPAR, and that the anthraquinone core (rings A–C) is engaged in hydrophobic interactions with residues L55, L123, L150, L168, V125, and A255 (Figure S7, Table S2). The two D ring sulfonates in ARM-U2 are positioned within 2.8 and 3.5 Å of R53 and T66,

respectively, suggesting the presence of close-range electrostatic and perhaps hydrogen-bonding contacts (Figure 4 A, B). These results suggest that enhanced polar contacts between the sulfonates present in ARM-U2 and hot-spot residues on uPAR are responsible for high-affinity binding.

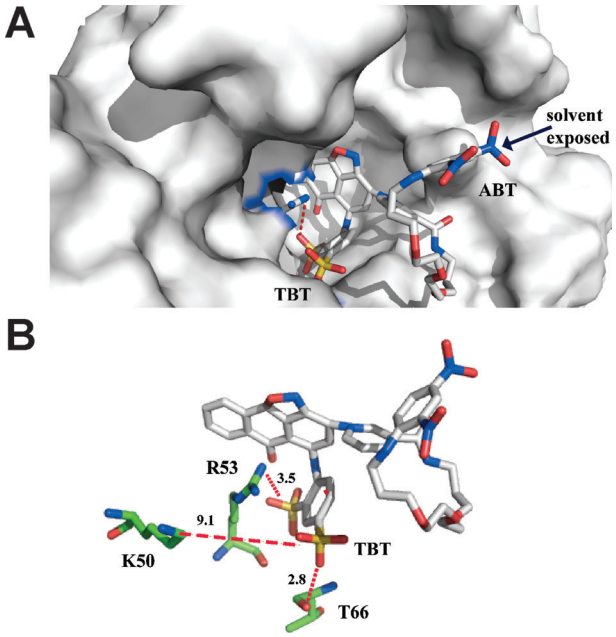

Figure 4. A, B) X-ray crystal structure of ARM-U2 bound to the uPA binding site of suPAR. Key interactions between the TBT sulfonates and the uPA binding-site residues R53 and T66 (distances of 3.5 and 2.8, respectively) are indicated with dotted red lines. In contrast to computational predictions, residue K50 is 9.1 Å away from the TBT, outside the hydrogen-bonding range.

Finally, we examined the efficacy of ARM-U2 in a B16-uPAR mouse allograft model developed in our laboratory. Mice were first immunized to produce anti-DNP IgG antibodies (Figure S8), then engrafted with B16-uPAR tumors as detailed in the Supporting Information. Animals received daily treatment with the indicated agents by intraperitoneal (IP) injection and were monitored for tumor growth. Mice treated with ARM-U2 (20 mpk or 100 mpk) showed significant decreases in the rate of tumor growth relative to those injected with PBS only, corresponding to a calculated tumor growth inhibition (TGI) of approximately 90 % (Figure 5 A). This level of TGI was comparable to mice treated with doxorubicin (Dox, 1 mpk), an antimitotic chemotherapeutic agent often used as a standard of care in treating metastatic malignancies, or a combination of ARM-U2 and Dox (20 mpk and 1 mpk, respectively). Furthermore, following treatment cessation, tumor regression persisted in all treatment groups for significantly longer than in the PBS control group (Figure 5 B). Specifically, median survival durations of between 27 and 37 days were observed for mice treated with Dox, ARM-U2, or a combination of these agents, whereas a median survival of 17.5 days was recorded for animals in the PBS control group. Remarkably, mice treated with ARM-U2 at either 20 or 100 mpk doses did not lose

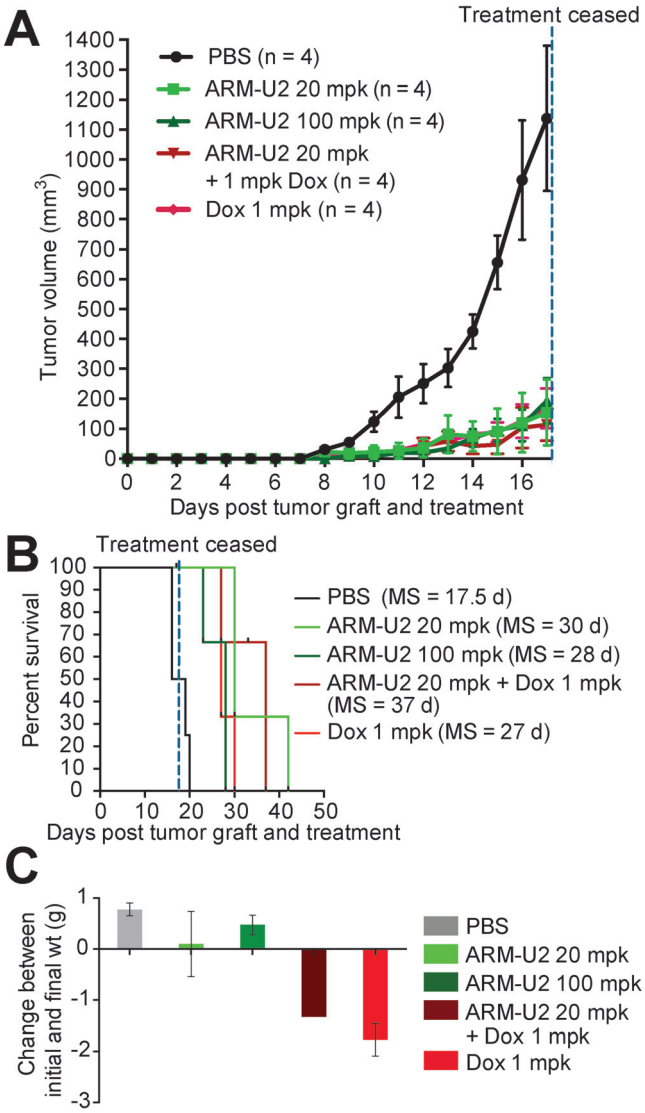

Figure 5. A) Tumor growth inhibition in a B16 mouse melanoma allograft model expressing human uPAR. Tumor growth is measured over the indicated timeframe upon daily treatment with PBS, doxorubicin at 1 mpk, combined doxorubicin (1 mpk)/ARM-U2 (20 mpk), or ARM-U2 at 20 mpk and 100 mpk in mice grafted with uPAR-expressing B16 melanoma cells. B) Kaplan–Meier curves demonstrating the prolongation of the survival of mice allografted with human uPAR-positive tumors upon treatment with ARM-U2 at both 20 mpk and 100 mpk, doxorubicin, or doxorubicin/ARM-U2 compared to mice treated with PBS. Dox = doxorubicin, mpk = milligrams per kilogram, MS = median survival (in days). C) Measured weight loss associated with ARM-U2 or doxorubicin treatment.

weight throughout the course of the experiments, in contrast to significant levels of weight loss observed among Dox-treated animals (Figure 5 C). Although lack of weight loss is not a definitive indicator of compound safety, these results represent a positive indication that ARM-U2 might possess an improved side-effect profile compared to doxorubicin.

In conclusion, we have developed a promising strategy for cancer immunotherapy that enables both the disruption of the oncogenic uPA–uPAR interaction and the ability to target uPAR-expressing cancers for immune-mediated cell death.

Although aryl sulfonates are uncommon in medicinal chemistry, we believe that the high negative charge of ARM-U2 plays an important role in its efficacy and potency, both in cellular assays and in vivo. Indeed, crystallographic studies indicate key interactions between sulfonic acid motifs in ARM-U2 and binding-site residues within uPAR lending both affinity and specificity to the interaction. Additional advantages of these charged groups might include reductions in off-target cellular binding and uptake, high aqueous solubility, and suppression of hydrophobic sticking and aggregation phenomena.

In vivo studies demonstrated that the tumor-killing efficacy of ARM-U2 was similar to that of doxorubicin, but without the weight loss associated with doxorubicin treatment. This observation may reflect an increase in selectivity associated with our targeted strategy as compared to traditional chemotherapeutics. Overall the ARM approach holds the exciting promise of combining the advantages of small-molecule and biologic therapeutic modalities, along with the hope for providing better treatments for patients with cancer.

Acknowledgements

We would like to thank Dr. Julian Vastl, Dr. Tina Wang, and Dr. Dianna Bartel for helpful suggestions in the preparation of this manuscript. D.A.S. is a paid consultant for Bristol-Myers Squibb. This work was supported by funding from Bristol-Myers Squibb (OCR4997.11 to D.A.S.). We also acknowledge grants from the NRF (2013R1A2A2A01067638 and 2012M3C1A6035362 to A.E.C.).

Keywords: antitumor agents · cell recognition · drug design · immunology · medicinal chemistry

How to cite: *Angew. Chem. Int. Ed.* **2016**, *55*, 3642–3646
Angew. Chem. **2016**, *128*, 3706–3710

[1] a) P. A. Andreasen, L. Kjoller, L. Christensen, M. J. Duffy, *Int. J. Cancer* **1997**, *72*, 1–22; b) M. J. Duffy, C. Duggan, *J. Natl. Cancer Inst.* **1997**, *89*, 1628–1629.

[2] a) M. J. Duffy, C. Duggan, T. Maguire, E. McDermott, N. O. Higgins, *Eur. J. Cancer* **1997**, *33*, 879–879; b) J. Romer, B. S. Nielsen, M. Ploug, *Curr. Pharm. Des.* **2004**, *10*, 2359–2376; c) F. Blasi, P. Carmeliet, *Nat. Rev. Mol. Cell Biol.* **2002**, *3*, 932–943; d) M. J. Duffy, *Fibrinolysis* **1993**, *7*, 295–302.

[3] a) S. Kennedy, M. J. Duffy, C. Duggan, C. Barnes, R. Rafferty, M. D. Kramer, *Br. J. Cancer* **1998**, *77*, 1638–1641; b) N. Harbeck, R. E. Kates, K. Gauger, A. Willems, M. Kiechle, V. Magdolen, M. Schmitt, *Thromb. Haemostasis* **2004**, *91*, 450–456.

[4] a) T. M. Allen, *Nat. Rev. Cancer* **2002**, *2*, 750–763; b) Y. J. Lu, P. S. Low, *J. Pharm. Pharmacol.* **2003**, *55*, 163–167; c) A. Jemal, R. Siegel, J. Q. Xu, E. Ward, *Ca-Cancer J. Clin.* **2010**, *60*, 277–300; d) P. X. Xing, I. F. C. Mckenzie, *Breast Epithelial Antigens: Molecular Biology to Clinical Applications*, Springer, New York, **1991**, 45–54; e) G. Ragupathi, T. K. Park, S. L. Zhang, I. J. Kim, L. Graber, S. Adluri, K. O. Lloyd, S. J. Danishefsky, P. O. Livingston, *Angew. Chem. Int. Ed. Engl.* **1997**, *36*, 125–128; *Angew. Chem.* **1997**, *109*, 66–69; f) C. Garbe, T. K. Eigentler, U. Keilholz, A. Hauschild, J. M. Kirkwood, *Oncologist* **2011**, *16*, 5–24; g) Y. J. Lu, P. S. Low, *Cancer Immunol. Immunother.* **2002**, *51*, 153–162; h) S. Vichier-Guerre, R. Lo-Man, L. BenMohamed, E. Deriaud, S. Kovats, C. Leclerc, S. Bay, *J. Pept. Res.* **2003**, *62*, 117–124; i) M. Popkov, B. Gonzalez, S. C. Sinha, C. F. Barbas, *Proc. Natl. Acad. Sci. USA* **2009**, *106*, 4378–4383; j) A. X. Zhang, R. P. Murelli, C. Barinka, J. Michel, A. Cocleaza, W. L. Jorgensen, J. Lubkowski, D. A. Spiegel, *J. Am. Chem. Soc.* **2010**, *132*, 12711–12716; k) D. A. Spiegel, *Expert Rev. Clin. Pharmacol.* **2013**, *6*, 223–225; l) R. P. Murelli, A. X. Zhang, J. Michel, W. L. Jorgensen, D. A. Spiegel, *J. Am. Chem. Soc.* **2009**, *131*, 17090–17092.

[5] a) C. E. Jakobsche, P. J. McEnaney, A. X. Zhang, D. A. Spiegel, *ACS Chem. Biol.* **2012**, *7*, 316–320; b) P. J. McEnaney, C. G. Parker, A. X. Zhang, D. A. Spiegel, *ACS Chem. Biol.* **2012**, *7*, 1139–1151.

[6] M. Khanna, F. Wang, I. Jo, W. E. Knabe, S. M. Wilson, L. W. Li, K. Bum-Erdene, J. Li, G. W. Sledge, R. Khanna, S. O. Meroueh, *ACS Chem. Biol.* **2011**, *6*, 1232–1243.

[7] Q. Huai, A. Zhou, L. Lin, A. P. Mazar, G. C. Parry, J. Callahan, D. E. Shaw, B. Furie, B. C. Furie, M. Huang, *Nat. Struct. Mol. Biol.* **2008**, *15*, 422–423.

[8] a) T. Mani, F. Wang, W. E. Knabe, A. L. Sinn, M. Khanna, I. Jo, G. E. Sandusky, G. W. Sledge, D. R. Jones, R. Khanna, K. E. Pollok, S. O. Meroueh, *Bioorg. Med. Chem.* **2013**, *21*, 2145–2155; b) F. Wang, W. E. Knabe, L. W. Li, I. Jo, T. Mani, H. Roehm, K. Oh, J. Li, M. Khanna, S. O. Meroueh, *Bioorg. Med. Chem.* **2012**, *20*, 4760–4773.

[9] E. F. Douglass, Jr., C. J. Miller, G. Sparer, H. Shapiro, D. A. Spiegel, *J. Am. Chem. Soc.* **2013**, *135*, 6092–6099.

[10] a) C. B. Marsh, C. L. Anderson, M. P. Lowe, M. D. Wewers, *J. Immunol.* **1996**, *157*, 2632; b) C. Shi, E. G. Pamer, *Nat. Rev. Immunol.* **2011**, *11*, 762–774.

[11] a) X. Xu, H. Gardsvoll, C. Yuan, L. Lin, M. Ploug, M. Huang, *J. Mol. Biol.* **2012**, *416*, 629–641; b) H. Gårdsvoll, M. Kjaergaard, B. Jacobsen, M. C. Kriegbaum, M. Huang, M. Ploug, *J. Biol. Chem.* **2011**, *286*, 43515–43526 .

Received: November 23, 2015
Revised: December 23, 2015
Published online: February 15, 2016

